Polymorphism in Spin Transition Systems. Crystal Structure, Magnetic Properties, and Mössbauer Spectroscopy of Three Polymorphic Modifications of [Fe(DPPA)(NCS)$_2$] [DPPA = (3-Aminopropyl)bis(2-pyridylmethyl)amine]

Galina S. Matouzenko,*,† Azzedine Bousseksou,‡ Sylvain Lecocq,§ Petra J. van Koningsbruggen,|| Monique Perrin,§ Olivier Kahn,|| and André Collet*,†

Stéréochimie et Interactions moléculaires (UMR CNRS and ENS-Lyon No. 117; chaire de l'Institut universitaire de France), École normale supérieure de Lyon, 46, allée d'Italie, 69364 Lyon cedex 07, France, Laboratoire de chimie de coordination (UPR CNRS No. 8241), 205, route de Narbonne, 31077 Toulouse cedex, France, and School of Chemistry, Queen's University of Belfast, Belfast, BT9 5AG, Northern Ireland, Laboratoire de reconnaissance et organisation moléculaire (ESA Q5078), Université Claude Bernard-Lyon 1, 69622 Villeurbanne cedex, France, and Laboratoire des sciences moléculaires, Institut de chimie de la matière condensée de Bordeaux (UPR CNRS No. 9048), 33608 Pessac, France

Received September 13, 1997[⊗]

Three polymorphic modifications A−C of [Fe^{II}(DPPA)(NCS)$_2$], where DPPA = (3-aminopropyl)bis(2-pyridylmethyl)amine is a new tetradentate ligand, have been synthesized, and their structures, magnetic properties, and Mössbauer spectra have been investigated. For polymorph A, variable-temperature magnetic susceptibility measurements as well as Mössbauer spectroscopy have revealed the occurrence of a rather gradual HS ⇔ LS transition without hysteresis, centered at about 176 K. The same methods have shown that polymorph B is paramagnetic over the temperature range 4.5−295 K, whereas polymorph C exhibits a very abrupt $S = 2 \Leftrightarrow S = 0$ transition with a hysteresis. The hysteresis width is 8 K, the transitions being centered at $T_c\downarrow = 112$ K for decreasing and $T_c\uparrow = 120$ K for increasing temperatures. The crystal structures of the three polymorphs have been solved by X-ray diffraction at 298 K. Polymorph A is triclinic, space group $P\bar{1}$ with $Z = 2$, $a = 8.710(2)$ Å, $b = 15.645(2)$ Å, $c = 7.985(1)$ Å, $\alpha = 101.57(1)°$, $\beta = 112.59(2)°$, and $\gamma = 82.68(2)°$. Polymorph B is monoclinic, space group $P2_1/c$ with $Z = 4$, $a = 8.936(2)$ Å, $b = 16.855(4)$ Å, $c = 13.645(3)$ Å, and $\beta = 97.78(2)°$. Polymorph C is orthorhombic, space group *Pbca* with $Z = 8$, $a = 8.449(2)$ Å, $b = 14.239(2)$ Å, and $c = 33.463(5)$ Å. In the three polymorphs, the asymmetric units are almost identical and consist of one chiral complex molecule with the same configuration and conformation. The distorted [FeN$_6$] octahedron is formed by four nitrogen atoms belonging to DPPA and two provided by the *cis* thiocyanate groups. The two pyridine rings of DPPA are in *fac* positions. The main differences between the structures of the three polymorphs are found in their crystal packing. The stabilization of the high-spin ground state of polymorph B is tentatively explained by the presence of two centers of steric strain in the crystal lattice resulting in the elongation of the Fe−N(aromatic) distance. The observed hysteresis in polymorph C seems to be due to the existence of an array of intermolecular contacts in the crystal lattice making the spin transition more cooperative than in polymorph A.

Introduction

Spin transition phenomena represent an important area of interest in iron(II) coordination chemistry.[1] In crystalline materials, the change of electronic states from high spin (HS, $S = 2$) to low spin (LS, $S = 0$) can be induced thermally or by such physical perturbations as pressure change or light irradiation. The proximity of high-spin and low-spin electronic states is a prerequisite for the occurrence of a spin transition. Although this energy gap can in principle be tuned in a relatively predictable fashion by variation of the ligand field force, this is not the only factor upon which the existence and character of a spin interconversion depend. The crystal structure plays a major role here, and this is why the existence of several polymorphic modifications of the same compound represents a particularly interesting situation for investigating spin transition phenomena, when it leads to different types of magnetic behavior which then can be analyzed in terms of molecular geometry and intermolecular interactions.

Only few systems have been reported so far to present such a behavior,[2−4] among which [Fe(bt)$_2$(NCS)$_2$,] (bt = 2,2′-bi-2-thiazoline), where one of the crystal forms shows a HS ⇔ LS transition whereas the other only possesses a high-spin state at the whole temperature range.[4] A variant of this situation is the co-existence in the same lattice of two crystallographically independent sites which exhibit different spin states. This uncommon issue is found in [Fe(mtz)$_6$](BF$_4$)$_2$ (mtz = 1-methyltetrazole), where one site is high-spin and the second undergoes a thermal spin transition.[5] It has also been reported for the iron(II) complex of a C$_3$-cyclotriveratrylene ligand,[6]

* Corresponding author.
† École normale supérieure de Lyon.
‡ Laboratoire de chemie de coordination and Queen's University Belfast.
§ Université Claude Bernard-Lyon 1.
|| Institute de chimie de la matère condensée de Bordeaux.
⊗ Abstract published in *Advance ACS Abstracts,* November 15, 1997.

(1) (a) Goodwin, H. A. *Coord. Chem. Rev.* **1976**, *18*, 293. (b) Gütlich, P. *Struct. Bonding* **1981**, *44*, 83. (c) König, E.; Ritter, G.; Kulshreshtha, S. K. *Chem. Rev.* **1985**, *85*, 219. (d) Toftlund, H. *Coord. Chem. Rev.* **1989**, *94*, 67. (e) Zarembowitch, J.; Kahn, O. *New J. Chem.* **1991**, *15*, 181. (f) König, E. *Struct. Bonding.* **1991**, *76*, 51. (g) Gütlich, P.; Hauser, A.; Spiering, H. *Angew. Chem., Int. Ed. Engl.* **1994**, *33*, 2024. (h) Kahn, O. *Molecular Magnetism*; VCH: New York 1993. (i) Kahn, O.; Codjovi, E. *Phil. Trans. R. Soc. Lond. A* **1996**, *354*, 359.
(2) König, E.; Madeja, K. *Inorg. Chem.* **1967**, *6*, 48.
(3) König, E.; Madeja, K.; Watson, K. J. *J. Am. Chem. Soc.* **1968**, *90*, 1146.
(4) Ozarowski, A.; McGarvey, B. R.; Sarkar, A. B.; Drake, E. *Inorg. Chem.* **1988**, *27*, 627.
(5) (a) Poganiuch, P.; Decurtins, S.; Gütlich, P. *J. Am. Chem. Soc.* **1990**, *112*, 3270. (b) Wiehl, L. *Acta Crystallogr.* **1993**, *B49*, 289.

S0020-1669(97)01174-9 CCC: $14.00

Chart 1. Representation of the DPEA and DPPA Ligands

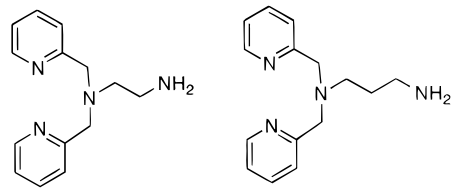

where one site is occupied by low-spin species whereas the other shows a temperature-independent mixture of high-spin and low-spin states.

We report here a striking example of the effect of polymorphism on spin transitions, in which *three* crystal forms of the same complex exhibit different magnetic properties. As shown earlier,[1d] ligands containing both aliphatic and aromatic nitrogen atoms feature intermediate ligand field force favoring the occurrence of spin-state interconversions. On the basis of this strategy, numerous complexes of polydentate ligands combining different types of nitrogen binding sites have been designed.[1a,d,7] Along these lines we have recently reported the synthesis of an iron(II) complex of the new tetradentate ligand (2-aminoethyl)-bis(2-pyridylmethyl)amine (DPEA) (Chart 1), containing two aliphatic and two aromatic nitrogen atoms.[8] The isolated *mer*-[Fe(DPEA)$(NCS)_2$] complex **1** was found to display a relatively sharp HS ⇔ LS transition at $T_{1/2}$ = 138 K. In **1**, the DPEA ligand coordinated to the iron(II) center forms three five-membered chelate metallocycles, resulting in a significant distortion of the coordination octahedron due to strain. Anticipating that enlargement of one of these metallocycles to a six-membered ring could somewhat reduce the strain and in turn modify the magnetic properties of the complex,[1d,7b,c] we have synthesized the new tetradentate ligand (3-aminopropyl)-bis(2-pyridylmethyl)amine (DPPA), which contains one more methylene unit in its aminoaliphatic chain (Chart 1). The corresponding *cis*-biisothiocyanate *fac*-[Fe(DPPA)$(NCS)_2$] complex **2** was actually isolated in the form of *three different polymorphic modifications*, A−C. These polymorphs were studied separately by temperature-dependent magnetic susceptibility measurements and Mössbauer spectroscopy, and their structures were established by single-crystal X-ray crystallography. Polymorph A undergoes a HS ⇔ LS transition at about 176 K, while B remains high-spin in the range 4.5−295 K and C shows a spin-state transition with hysteresis. Comparison of the crystal structures of these three forms showed that these differences are mostly due to crystal packing effect rather than to changes in the complex geometry, even though small differences in the Fe−N intramolecular distances and in the conformations of the chelate rings have also been evidenced.

Experimental Section

Chemistry. All reagents and solvents used in this study are commercially available and were used without further purification. [Fe$(py)_4(NCS)_2$] (py = pyridine) was prepared as described previously.[9] Bis(2-pyridylmethyl)amine (DPA) was obtained according to the procedure we recently reported.[8] All syntheses involving Fe(II) species were carried out in deoxygenated solvents under an inert atmosphere of N_2 using glovebox techniques. Elemental analyses (C, H, N, S, and Fe determination) were performed at the Service Central de Microanalyse du CNRS in Vernaison, France. ^{1}H NMR spectra were recorded in $CDCl_3$ on a Bruker AC200 spectrometer operating at 200 MHz.

(a) Ligand Synthesis. (3-Aminopropyl)bis(2-pyridylmethyl)-amine (DPPA). A mixture of DPA (8 g, 0.04 mol), triethylamine (5.6 mL, 0.04 mol), and *N*-(3-bromopropyl)phthalimide (10.7 g, 0.04 mol) in toluene (50 mL) was refluxed under argon overnight. Then the resulting precipitate was filtered off and the filtrate was concentrated under vacuum. The residue was extracted with ether, and the ethereal solution was dried over anhydrous $MgSO_4$. After evaporation of the ether 12.5 g (81%) of crude *N*-(3-bis(2-pyridylmethyl)propyl)phthalimide was obtained (red brown oil). ^{1}H NMR ($CDCl_3$): δ 8.46−7.04 (m, 8H, aromatic H's), 7.81−7.48 (m, 4H, aromatic H's), 3.79 (s, 4H, CH_2), 3.71−3.63 (t, 2H, CH_2), 2.64−2.57 (t, 2H, CH_2), 1.96−1.82 (m, 2H, CH_2). To this product dissolved in 50 mL of absolute ethanol was added 1.57 mL (0.032 mol) of hydrazine monohydrate. The mixture was refluxed under argon until formation of a white gelatinous precipitate. When the formation of the latter appeared complete, it was decomposed by heating with 12 M HCl (15 mL). The precipitate (phthalohydrazide hydrochloride) was filtered off, and the solution was concentrated under vacuum. The residue was made basic with aqueous NaOH, and the organic material was extracted with ether. The ethereal solution was dried over KOH pellets and evaporated under vacuum to give 6 g (59%) of essentially pure DPPA (yellow oil). ^{1}H NMR ($CDCl_3$): δ 8.50−7.08 (m, 8H, aromatic H's), 3.78 (s, 4H, CH_2), 2.89−2.52 (m, 4H, CH_2), 1.70−1.59 (m, 2H, CH_2), 1.10 (s, 2H, NH_2).

(b) Synthesis of the Iron(II) Complexes. The three polymorphs A−C were prepared from a solution of [Fe$(py)_4(NCS)_2$] (48.8 mg, 0.1 mmol) in 10 mL of absolute ethanol, which was mixed with 25.5 mg (0.1 mmol) of DPPA in 5 mL of absolute ethanol. The resulting yellow solution was allowed to crystallize at room temperature in a glovebox. In most experiments, the crystallization was observed to occur after about 2 h, yielding long yellow brown prismatic crystals of a EtOH solvated form of the complex.[10] In some cases however the crystallization occurred only after 5−7 days, yielding the polymorphs A−C, pure or as mixtures of crystals of different types which were separated under microscope. Polymorph A formed yellow green plates, B was isolated as yellow prisms, and C was isolated as pale yellow elongated hexagonal plates. The crystals were filtered off, washed with ethanol, and dried in vacuum. These three polymorphs were suitable for single-crystal X-ray studies. Anal. Calcd for $C_{17}H_{20}N_6S_2Fe$: C, 47.67; H, 4.71; N, 19.62; S, 14.97; Fe, 13.04. Found for polymorph A: C, 47.77; H, 4.86; N, 19.75; S, 14.91; Fe, 13.08. Found for polymorph B: C, 47.25; H, 4.60; N, 19.77; S, 14.84; Fe, 13.22. Polymorph C was not analyzed due to the lack of material.

Physical Measurements. (a) Magnetic Properties. Magnetic susceptibilities of polymorph A were measured in the range 5−300 K with a fully automated Manics DSM-8 susceptometer equipped with a TBT continuous-flow cryostat and a Drusch EAF 16 UE electromagnet operating at ca. 1.7 T. Magnetic susceptibilities were measured for polymorphs B and C in the temperature range 2−300 and 2−190 K, respectively, on a quantum design MPMS-5S SQUID magnetometer (Princeton Applied Research PAR 151) equipped with a Bruker electromagnet operating at 1 T and a CryoVac liquid-helium cryostat. Data were corrected for magnetization of the sample holder and for diamagnetic contributions, which were estimated from the Pascal constants.

(b) Mössbauer Spectra. The variable-temperature Mössbauer measurements were obtained on a constant-acceleration spectrometer with a 25 mCi source of ^{57}Co (Rh matrix). The isomer shift values (IS) are given with respect to metallic iron at room temperature. The absorber was a sample of microcrystalline powder enclosed in a 2 cm diameter cylindrical plastic sample holder, the size of which had been determined to optimize the absorption. The variable-temperature spectra

(6) Matouzenko, G.; Vériot, G.; Dutasta, J. P.; Collet, A.; Jordanov, J.; Varret, F., Perrin, M., Lecocq, S. *New J. Chem.* **1995**, *19*, 881.
(7) (a) Toftlund, H.; Yde-Andersen, S. *Acta Chem. Scand. A* **1981**, *35*, 575. (b) Højland, F.; Toftlund, H.; Yde-Andersen, S. *Acta Chem. Scand. A* **1983**, *37*, 251. (c) Toftlund, H.; Pedersen, E.; Yde-Andersen, S. *Acta Chem. Scand. A* **1984**, *38*, 693. (d) Chang, H. R.; McCusker, J. K.; Toftlund, H.; Wilson, S. R.; Trautwein, A. X.; Winkler, H.; Hendrickson, D. N. *J. Am. Chem. Soc.* **1990**, *112*, 6814. (e) McCusker, J. K.; Toftlund, H.; Rheingold, A. L.; Hendrickson, D. N. *J. Am. Chem. Soc.* **1993**, *115*, 1797. (f) Al-Obaidi, A. H. R.; McGarvey, J. J.; Taylor, K. P.; Beel, S. E. J.; Jensen, K. B.; Toftlund, H. *J. Chem. Soc. Chem. Comm.* **1993**, 536. (g) McCusker, J. K.; Rheingold, A. L.; Hendrickson, D. N. *Inorg. Chem.* **1996**, *35*, 2100. (h) Al-Obaidi, A. H. R.; Jensen, K. B.; McGarvey, J. J.; Toftlund, H.; Jensen, B.; Beel, S. E. J., Carroll, J. G. *Inorg. Chem.* **1996**, *35*, 5055.
(8) Matouzenko, G. S.; Bousseksou, A.; Lecocq, S.; Koningsbruggen, P. J. van.; Perrin, M.; Kahn, O.; Collet, A. *Inorg. Chem.*. **1997**, *36*, 2975.
(9) Erickson, N. E.; Sutin, N. *Inorg.Chem.* **1966**, *5*, 1834.
(10) The solvated complex [Fe(DPPA)$(NCS)_2$]·0.5$C_2H_5$0H is under study now and will be presented in a future publication.

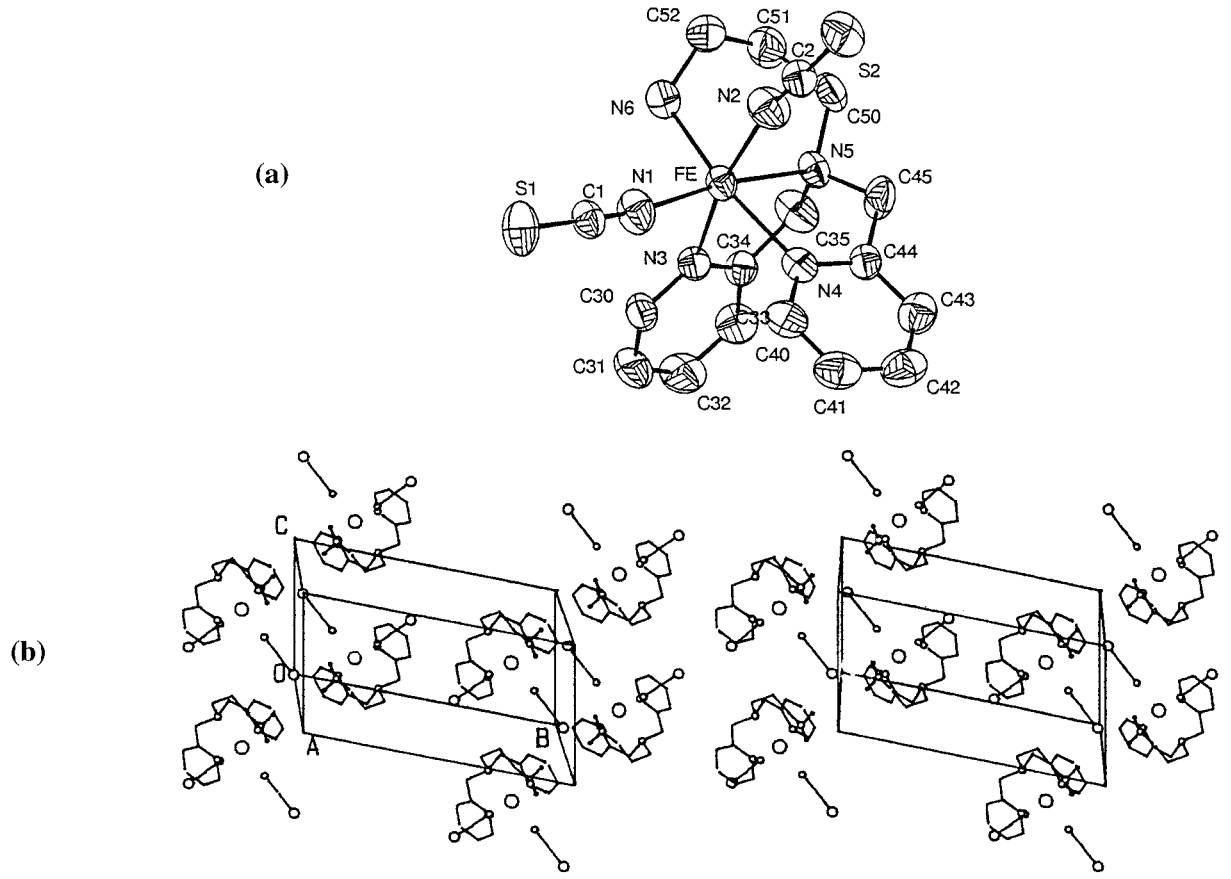

Figure 1. (a) Perspective view of the *fac*-[Fe(DPPA)(NCS)$_2$] (**2**) molecule in polymorph A (ellipsoids enclose 50% probability). (b) Stereoview of the packing diagram for polymorph A.

Table 1. Crystallographic Data for *fac*-[Fe(DPPA)(NCS)$_2$] in Polymorphs A−C

	A	B	C
chem formula	$C_{17}H_{20}N_6S_2Fe$	$C_{17}H_{20}N_6S_2Fe$	$C_{17}H_{20}N_6S_2Fe$
a, Å	8.710(2)	8.936(2)	8.449(2)
b, Å	15.645(2)	16.855(4)	14.239(2)
c, Å	7.985(1)	13.645(3)	33.463(5)
α, deg	101.57(1)	90.0	90.0
β, deg	112.59(2)	97.78(2)	90.0
γ, deg	82.68(2)	90.0	90.0
V, Å^3	982.6(3)	2036.2(9)	4026(1)
Z	2	4	8
fw	428.35	428.35	428.35
space group	$P\bar{1}$	$P2_1/c$	*Pbca*
temp, K	298	298	298
λ (Cu Kα), Å	1.540 56	1.540 56	1.540 56
ρ_{calc}, g·cm^{-3}	1.448	1.397	1.413
μ, cm^{-1}	82.48	79.61	80.53
R^a	0.069	0.060	0.058
$R_w{}^b$	0.069	0.066	0.065

^{a} $R = \sum(|F_o| - |F_c|)/\sum|F_o|$. ^{b} $R_w = [\sum w(|F_o| - |F_c|)^2/\sum w|F_o|^2]^{1/2}$.

were obtained in the range 80−305 K, by using a MD306 Oxford cryostat, the thermal scanning being monitored by an Oxford ITC4 servocontrol device (±0.1 K). A least-squares computer program was used to fit the Mössbauer parameters and determine their standard deviations of statistical origin (given in parentheses).[11]

(c) Solution and Refinement of the X-ray Structure. The structures of the three polymorphs of the above described complex were determined at room temperature (ca. 298 K). The crystals were sealed in a Lindemann capillary and mounted on a four-circle diffractometer (CAD4 Enraf-Nonius) with Cu anticathode. Crystal data and refinement results are summarized in Table 1. Cell parameters were determined from 25 reflections. For each compound three reflections were measured every 1 h as a control of the crystal quality and every 100 reflections as an intensity control. The SDP[12] package supplied by

Chart 2. Stereoisomers **2** and **3** of [Fe(DPPA)(NCS)$_2$],[a] the Structure of *mer*-[Fe(DPEA)(NCS)$_2$] (**1**) Shown for Comparison

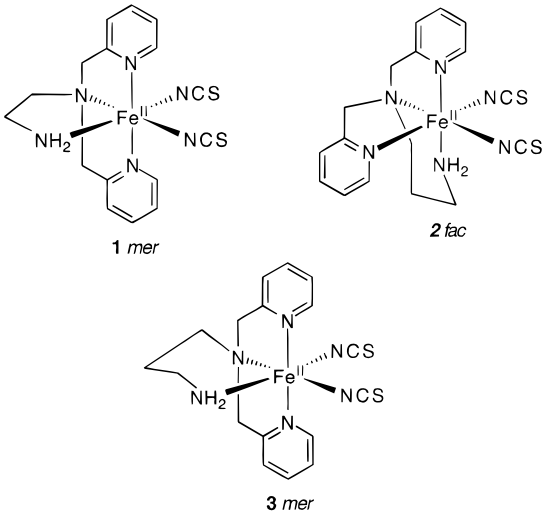

[a] Only **2** where the pyridine ligands are facially arranged was isolated in this work.

Nonius was used to correct the intensities from absorption and usual Lorentz polarization; MULTAN[13] gave the hypothesis by direct methods, and the SHELX-76 program[14] was used for the refinement by full-matrix least-squares methods. Non-hydrogen atoms were refined anisotropically; all hydrogen atoms were refined isotropically. Hydrogen coordinates, anisotropic thermal parameters of non-hydrogen

(11) Varret, F. *Proceedings of the International Conference on Mössbauer Effect Applications*; Jaipar, India, 1981; Indian National Science Academy: New Delhi, 1982.
(12) Frenz, B. A. *Stucture determination package*; Enraf-Nonius: Delft, The Netherlands, 1982.

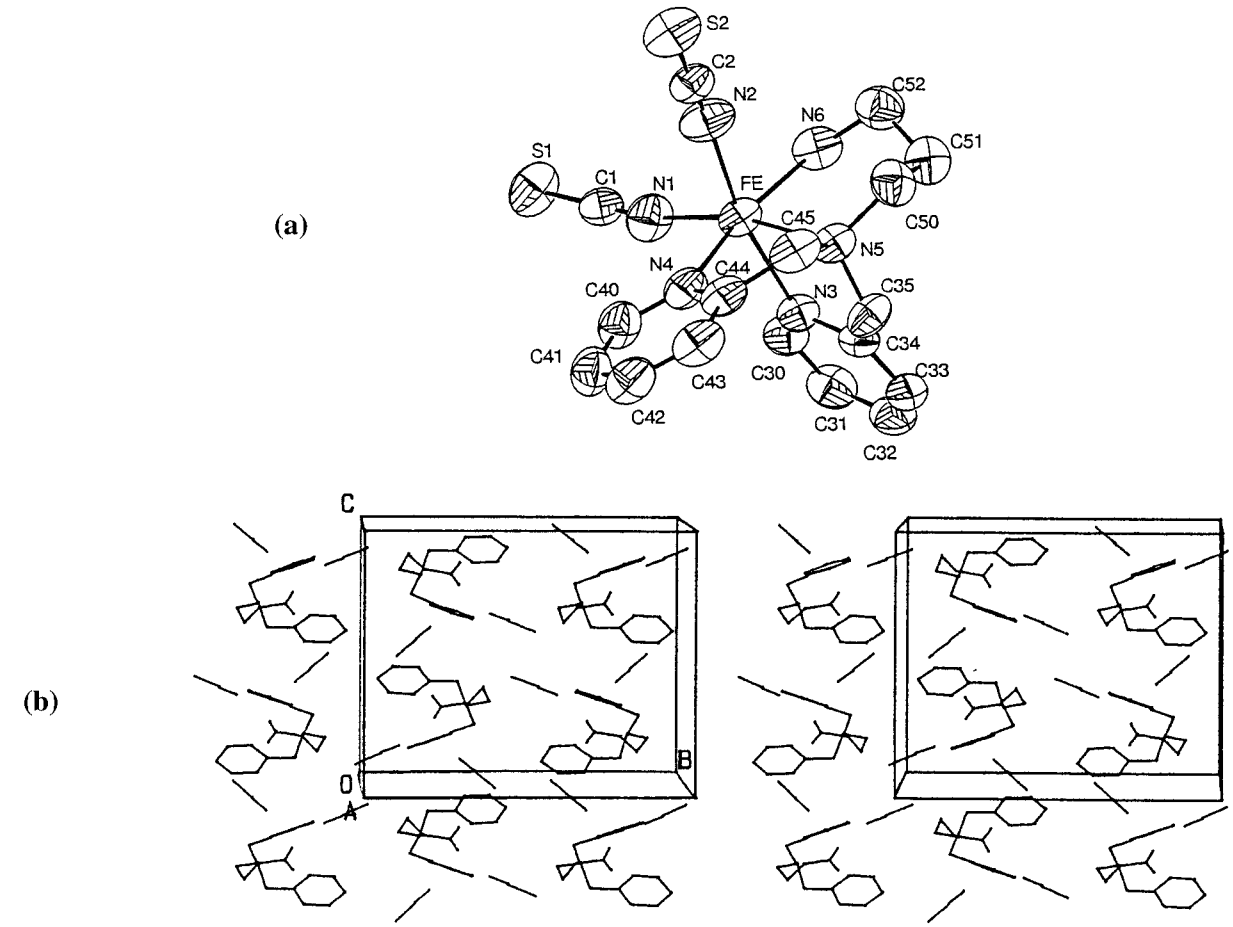

Figure 2. (a) Perspective view of the *fac*-[Fe(DPPA)(NCS)$_2$] (**2**) molecule in polymorph B (ellipsoids enclose 50% probability). (b) Stereoview of the packing diagram for polymorph B.

atoms, remaining bond distances and angles, and least-square planes are deposited as Supporting Information.

Results

Structural Descriptions. (a) Stereochemistry. Octahedral [Fe(DPPA)(NCS)$_2$] complexes comprise one six-membered chelate ring formed by the aliphatic propanediamine chain and two five-membered rings resulting from the coordination of the (pyridylmethyl)amino fragments of the tetradentate ligand (Chart 2). Although in principle a variety of isomers can exist, the four nitrogen atoms of DPPA must occupy two apical and two adjacent equatorial positions in the octahedron to avoid strain that would result from three meridionally fused chelates. This makes the *cis* arrangement of the two NCS groups the only possible. The two pyridine rings of the ligand can have either facial or meridional arrangement (**2** and **3**, respectively, in Chart 2). The *mer* configuration is achiral (due to the flexibility of the six-membered ring) whereas the *fac* arrangement leads to a chiral complex resolvable into enantiomers. In contrast with our previous work where only the *mer* configuration **1** was isolated from the DPEA ligand, in all three polymorphs isolated in this work only the *fac* arrangement **2** of the pyridine ligands is realized. The six-membered propanediamine metallocycle is in the *chair* conformation.[15] Disregarding small differences in bond lengths and angles (which will be discussed later) the conformation of complex **2** is nearly the same in the three polymorphs and represents the asymmetric units in the three crystal structures (Figures 1−3).

(b) Crystal Structure of Polymorph A. This form crystallizes in the $P\bar{1}$ triclinic space group. The unit cell contains one pair of enantiomeric *fac*-[Fe(DPPA)(NCS)$_2$] molecules **2** (Z = 2). The perspective view of the molecule is shown in Figure 1a. Fractional atomic coordinates and selected bond lengths and angles are given in Tables 2−4, respectively.

In this structure, the [FeN$_6$] octahedron is strongly distorted. The Fe−N distances involving the pyridine rings (Fe−N3 = 2.209(3) Å, Fe−N4 = 2.182(4) Å) and the aliphatic amino groups (Fe−N5 = 2.284(4) Å, Fe−N6 = 2.182(5) Å) are longer than those involving the two thiocyanate groups (Fe−N1 = 2.084(6) Å, Fe−N2 = 2.103(4) Å). The Fe−N5 distance is significantly longer than all other Fe−N distances. The N−Fe−N angles between the adjacent and opposite nitrogen atoms fall within the range 77.0(2)−98.2(2) and 163.4(2)−171.2(2)° instead of 90 and 180° for an ideal octahedron. The angles formed by the nitrogen atoms of the five-membered rings (N3−Fe−N5, N4−Fe−N5) as well as this between the two pyridine nitrogen atoms (N3−Fe−N4) are distinctly smaller than 90° (see Table 4). The angle between the nitrogen atoms of the six-membered ring (N5−Fe−N6) is much less reduced, probably due to the flexibility of the amino aliphatic chain. As a result of the reduction of the N−Fe−N angles associated with the DPPA ligand, the angles formed by the thiocyanate N1 atom and the atoms in *cis* positions are larger than 90°. Evidently, this distortion of the [FeN$_6$] core from O_h symmetry is due to the steric constraints caused by the coordination of the tetraden-

(13) Main, P.; Fiske, S. J.; Hull, S. E.; Lessinger, L.; Germain, G.; Declercq, J. P.; Woolfson, M. M. *MULTAN 80, A System of Computer Programs for the Automatic solution of Crystal Structure from X-ray Diffraction Data*; University of York, England, and University of Louvain, Belgium, 1980.
(14) Sheldrick, G. M. *SHELX-76, Computer Program for Crystal Structure Determination*; University of Cambridge: England, 1976.

(15) In previously structurally characterized complexes the six-membered propanediamine chelate ring can adopt in the solid state either *a, p chair* or *λ, δ twist-boat* conformations.

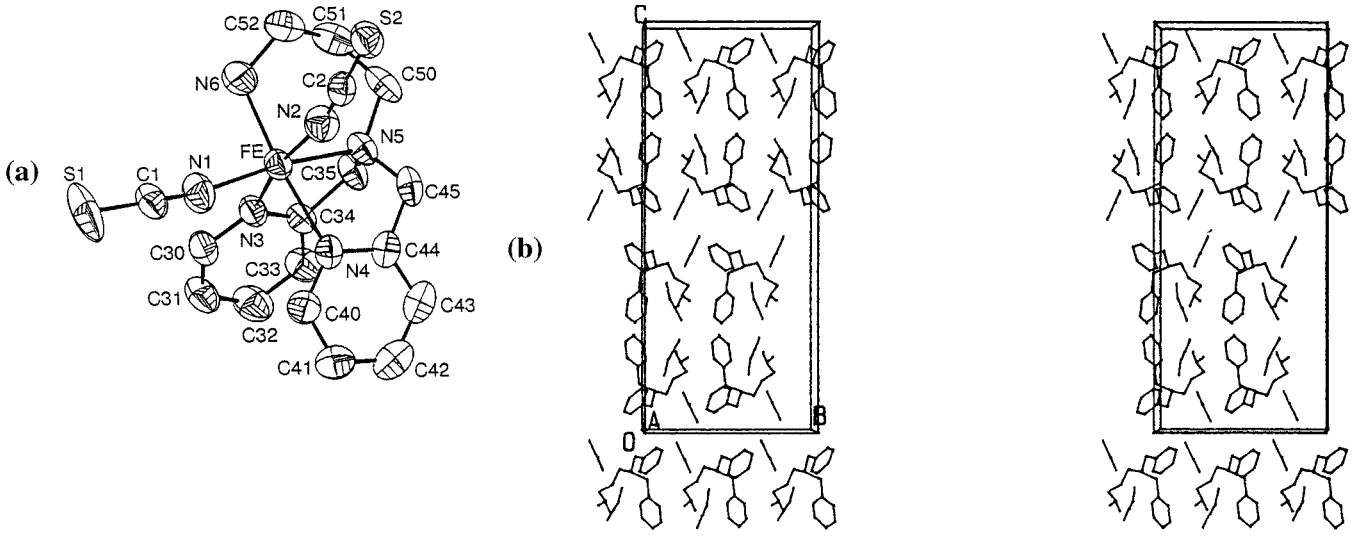

Figure 3. (a) Perspective view of the *fac*-[Fe(DPPA)(NCS)$_2$] (**2**) molecule in polymorph C (ellipsoids enclose 50% probability). (b) Stereoview of the packing diagram for polymorph C.

Table 2. Fractional Atomic Coordinates and Isotropic Equivalent Displacement Parameter[a,b] for Non-Hydrogen Atoms for *fac*-[Fe(DPPA)(NCS)$_2$] in Polymorphs A−C

atom	*x/a*	*y/b*	*z/c*	B_{eq}, Å^2	atom	*x/a*	*y/b*	*z/c*	B_{eq}, Å^2
		Polymorph A			C35	0.4678(6)	0.2959(2)	0.3924(3)	4.1(1)
Fe	0.23689(9)	0.22253(5)	0.30126(9)	3.02(2)	N5	0.5380(4)	0.3221(2)	0.3050(3)	3.84(8)
S1	0.2724(2)	0.0247(1)	0.7126(2)	5.61(5)	C50	0.6444(7)	0.3891(3)	0.3337(4)	5.2(1)
N1	0.2303(6)	0.1376(3)	0.4685(6)	4.8(1)	C51	0.7889(7)	0.3643(4)	0.4001(4)	5.8(1)
C1	0.2462(6)	0.0906(3)	0.5693(7)	3.7(1)	C52	0.9007(6)	0.3190(3)	0.3495(4)	5.3(1)
S2	0.6130(2)	0.4144(1)	0.8063(2)	5.31(4)	N6	0.8507(5)	0.2357(2)	0.3271(3)	4.61(9)
N2	0.4222(6)	0.2987(3)	0.5096(6)	4.7(1)	N4	0.4017(4)	0.2160(2)	0.1614(3)	3.87(8)
C2	0.4992(6)	0.3467(3)	0.6340(6)	3.5(1)	C40	0.3250(5)	0.1517(3)	0.1258(4)	4.5(1)
N3	0.0252(5)	0.1667(2)	0.0603(5)	3.10(9)	C41	0.1708(6)	0.1497(3)	0.1090(4)	5.2(1)
C30	−0.0656(6)	0.1043(3)	0.0601(7)	3.7(1)	C42	0.0909(6)	0.2153(4)	0.1300(4)	5.7(1)
C31	−0.2119(7)	0.0798(4)	−0.0862(8)	4.7(2)	C43	0.1677(6)	0.2823(3)	0.1671(4)	5.1(1)
C32	−0.2645(7)	0.1239(4)	−0.2331(8)	5.0(2)	C44	0.3229(5)	0.2805(3)	0.1834(3)	4.1(1)
C33	−0.1731(7)	0.1880(4)	−0.2348(7)	4.5(1)	C45	0.4171(6)	0.3490(3)	0.2263(4)	4.5(1)
C34	−0.0258(6)	0.2086(3)	−0.0848(6)	3.1(1)					
C35	0.0828(7)	0.2743(4)	−0.0889(7)	4.6(2)			Polymorph C		
N5	0.2017(5)	0.3123(2)	0.0948(5)	3.2(1)	Fe	0.35542(9)	0.12781(5)	0.13569(2)	3.91(2)
C50	0.3585(6)	0.3310(3)	0.0766(7)	3.9(1)	S1	0.7815(2)	0.2069(1)	0.22554(4)	6.16(4)
C51	0.4652(8)	0.2513(4)	0.0316(9)	4.8(2)	N1	0.5414(5)	0.1459(3)	0.1751(1)	5.4(1)
C52	0.5392(7)	0.1934(4)	0.1768(9)	4.8(2)	C1	0.6413(6)	0.1706(3)	0.1961(1)	4.2(1)
N6	0.4132(5)	0.1439(3)	0.1914(6)	3.9(1)	S2	0.4848(2)	0.3183(1)	0.02185(4)	6.12(4)
N4	0.0431(5)	0.3182(3)	0.3404(5)	3.3(1)	N2	0.4176(6)	0.2341(3)	0.0946(1)	5.7(1)
C40	−0.0545(7)	0.3105(4)	0.4322(7)	4.1(1)	C2	0.4468(6)	0.2688(3)	0.0640(1)	4.3(1)
C41	−0.1795(7)	0.3709(4)	0.4433(8)	4.9(2)	N3	0.2407(5)	0.0172(2)	0.17200(9)	3.83(8)
C42	−0.2102(7)	0.4415(4)	0.3549(8)	5.1(2)	C30	0.2676(7)	0.0050(3)	0.2112(1)	4.5(1)
C43	−0.1131(7)	0.4498(4)	0.2577(7)	4.5(1)	C31	0.1756(7)	−0.0530(4)	0.2346(2)	5.3(1)
C44	0.0142(6)	0.3876(3)	0.2554(6)	3.3(1)	C32	0.0501(7)	−0.0989(4)	0.2170(2)	5.3(1)
C45	0.1342(7)	0.3969(3)	0.1679(8)	4.5(2)	C33	0.0198(6)	−0.0860(3)	0.1772(2)	4.6(1)
					C34	0.1159(5)	−0.0259(3)	0.1555(1)	3.70(9)
		Polymorph B			C35	0.0934(7)	−0.0138(4)	0.1116(1)	4.6(1)
Fe	0.63899(7)	0.21917(4)	0.23193(5)	3.54(1)	N5	0.1629(5)	0.0737(3)	0.0946(1)	4.06(8)
S1	0.8276(3)	−0.02359(8)	0.1110(2)	9.32(6)	C50	0.0358(7)	0.1451(4)	0.0861(2)	5.2(1)
N1	0.7002(5)	0.1136(2)	0.1724(3)	5.3(1)	C51	−0.0387(7)	0.1874(4)	0.1232(2)	5.5(1)
C1	0.7522(5)	0.0565(3)	0.1471(4)	4.6(1)	C52	0.0593(7)	0.2637(4)	0.1433(2)	5.5(1)
S2	0.8744(1)	0.40058(7)	0.0215(1)	5.10(3)	N6	0.1917(5)	0.2248(3)	0.1664(1)	4.8(1)
N2	0.7104(5)	0.2945(2)	0.1219(3)	4.9(1)	N4	0.4715(5)	0.0219(3)	0.0980(1)	4.38(9)
C2	0.7780(5)	0.3400(3)	0.0797(3)	4.0(1)	C40	0.6107(7)	−0.0199(4)	0.1057(2)	5.2(1)
N3	0.5266(4)	0.1606(2)	0.3511(3)	3.67(8)	C41	0.6728(7)	−0.0887(4)	0.0813(2)	5.8(1)
C30	0.5070(6)	0.0820(3)	0.3570(4)	4.4(1)	C42	0.5911(8)	−0.1158(4)	0.0477(2)	5.9(1)
C31	0.3905(6)	0.0495(3)	0.4010(4)	5.1(1)	C43	0.4485(8)	−0.0732(4)	0.0396(2)	5.4(1)
C32	0.2921(6)	0.0988(3)	0.4388(4)	5.4(1)	C44	0.3934(6)	−0.0029(3)	0.0647(1)	4.4(1)
C33	0.3120(6)	0.1794(3)	0.4344(4)	4.6(1)	C45	0.2430(7)	0.0498(4)	0.0570(1)	4.8(1)
C34	0.4326(5)	0.2083(2)	0.3917(3)	3.53(9)					

[a] Estimated standard deviations in the least significant digits are given in parentheses. [b] $B_{eq} = {}^4/_3\sum_i\sum_j\beta_{ij}a_ia_j$.

tate DPPA ligand. The same features have been observed for *mer*-[Fe(DPEA)(NCS)$_2$] containing a similar tetradentate ligand[8] as well as for [FeL$_2$(NCS)$_2$] complexes containing bidentate ligands.[16] The NCS groups are almost linear (N1−C1−S1 = 178.9(5)°, N2−C2−S2 = 177.9(6)°), whereas the Fe−N−C linkages are appreciably bent (Fe−N1−C1 = 172.2(5)°, Fe−N2−C2 = 167.1(5)°). The pyridine rings of DPPA in polymorph A are nearly planar. The largest deviation from planarity in the N3 containing pyridine ring (mean plane 0.6565*x* − 0.6157*y* − 04359*z* = −1.4964) is found for atom C31 (0.009

Table 3. Selected Bond Distances (Å) for *fac*-[Fe(DPPA)(NCS)$_2$] in Polymorphs A−C[a]

	A	B	C
Fe−N1	2.084(6)	2.061(4)	2.067(5)
Fe−N2	2.103(4)	2.128(4)	2.112(4)
Fe−N3	2.209(3)	2.251(4)	2.213(3)
Fe−N5	2.284(4)	2.250(4)	2.266(4)
Fe−N6	2.182(5)	2.162(4)	2.208(4)
Fe−N4	2.182(4)	2.208(3)	2.197(4)
S1−C1	1.623(6)	1.616(5)	1.625(5)
N1−C1	1.155(8)	1.141(6)	1.154(6)
S2−C2	1.622(4)	1.613(5)	1.610(5)
N2−C2	1.148(6)	1.175(6)	1.162(6)
N3−C30	1.331(7)	1.340(5)	1.342(5)
N3−C34	1.344(6)	1.336(5)	1.339(6)
C30−C31	1.391(6)	1.383(8)	1.379(8)
C31−C32	1.376(9)	1.362(8)	1.378(8)
C32−C33	1.36(1)	1.372(7)	1.368(7)
C33−C34	1.398(6)	1.381(7)	1.384(6)
C34−C35	1.496(9)	1.510(6)	1.493(6)
C35−N5	1.489(5)	1.487(6)	1.490(7)
N4−C40	1.347(8)	1.338(6)	1.342(7)
N4−C44	1.341(7)	1.350(6)	1.344(6)
C40−C41	1.365(8)	1.367(7)	1.380(8)
C41−C42	1.37(1)	1.367(8)	1.375(9)
C42−C43	1.38(1)	1.382(8)	1.376(9)
C43−C44	1.382(7)	1.375(7)	1.385(7)
C44−C45	1.50(1)	1.500(6)	1.498(8)
N5−C45	1.481(7)	1.486(6)	1.469(6)
N5−C50	1.497(8)	1.494(6)	1.506(7)
C50−C51	1.527(8)	1.531(8)	1.517(8)
C51−C52	1.509(9)	1.498(8)	1.521(8)
C52−N6	1.473(9)	1.492(7)	1.469(7)

[a] Estimated standard deviations in the least significant digits are given in parentheses.

Å). The largest deviation observed in the N4 containing pyridine plane (mean plane $-0.4086x - 0.3879y - 0.8262z = -3.7852$) is 0.011 Å for atom C43. The dihedral angle between the two pyridinic planes in polymorph A is 70.7(2)°.

The crystal packing of polymorph A consists of layers of molecules parallel to the *ac* plane (Figure 1b). The cohesion within a layer is achieved by weak hydrogen bonds and van der Waals interactions between the molecules. The H-bond pattern is formed between H61 (belonging to N6) and the thiocyanate S1 of an adjacent molecule. Another H-bond network can also be suspected from the short S1···N6 contact (3.52 Å) (Table 6) formed by the same sulfur atom and the nitrogen atom of the molecule resulting from symmetry operation ($-x, -y, -z$). However, the position of H61 does not allow a linear arrangement of S···H−N. In the *b* direction, the cohesion is mainly due to the C42···C43 intermolecular contacts between the pyridine rings of adjacent layers. H-bonds and intermolecular distances (shorter than 3.6 Å for C···C contacts and 3.8 Å for C···S contacts) for polymorph A are summarized in Tables 5 and 6, respectively.

(c) Crystal Structure of Polymorph B. This form crystallizes in the monoclinic $P2_1/c$ space group. The unit cell contains two pairs of enantiomeric *fac*-[Fe(DPPA)(NCS)$_2$] molecules **2** ($Z = 4$). A perspective view of the molecule is shown in Figure 2a. Fractional atomic coordinates, selected bond lengths and angles are listed in Tables 2−4, respectively.

The [FeN$_6$] octahedron in polymorph B displays the same type of distortion as that observed in polymorph A, although

(16) (a) Gallois, B.; Real, J. A. Hauw, C.; Zarembowitch, J. *Inorg. Chem.* **1990**, *29*, 1152. (b) Claude, R.; Real, J. A., Zarembowitch, J.; Kahn, O.; Ouahab, L.; Grandjean, D.; Boukheddaden, K.; Varret, F.; Dworkin, A. *Inorg. Chem.* **1990**, *29*, 4442. (c) Granier, T.; Gallois, B.; Gaultier, J.; Real, J. A.; Zarembowitch, J. *Inorg Chem.* **1993**, *32*, 5305. (d) Real, J. A.; Muñoz, M. K.; Andrés, E.; Granier, T.; Gallois, B. *Inorg. Chem.* **1994**, *33*, 3587.

Table 4. Selected Angles (deg) for *fac*-[Fe(DPPA)(NCS)$_2$] in Polymorphs A−C[a]

	A	B	C
N1−Fe−N2	95.3(2)	96.6(2)	97.9(2)
N1−Fe−N3	94.5(2)	94.3(2)	94.1(2)
N1−Fe−N5	171.2(2)	169.9(2)	167.3(2)
N1−Fe−N6	97.4(2)	95.2(2)	95.8(2)
N1−Fe−N4	98.2(2)	95.6(1)	96.4(2)
N2−Fe−N3	168.7(2)	167.5(1)	167.6(2)
N2−Fe−N5	92.1(2)	91.7(1)	91.5(2)
N2−Fe−N6	93.5(2)	91.5(2)	90.6(2)
N2−Fe−N4	90.7(2)	93.9(1)	90.4(2)
N3−Fe−N5	77.7(1)	76.9(1)	77.1(1)
N3−Fe−N6	90.8(1)	93.6(1)	85.1(1)
N3−Fe−N4	82.3(1)	79.0(1)	91.3(1)
N5−Fe−N6	86.8(2)	90.3(1)	92.6(1)
N5−Fe−N4	77.0(2)	78.0(1)	74.9(1)
N6−Fe−N4	163.4(2)	167.3(2)	167.4(2)
Fe−N1−C1	172.2(5)	170.8(4)	169.4(4)
Fe−N2−C2	167.1(5)	163.4(3)	158.6(4)
S1−C1−N1	178.9(5)	179.3(5)	179.2(4)
S2−C2−N2	177.9(6)	178.4(4)	178.9(5)
Fe−N3−C30	124.6(3)	123.5(3)	123.7(3)
Fe−N3−C34	115.3(3)	113.8(2)	116.5(3)
C30−N3−C34	119.4(4)	118.3(4)	118.4(4)
Fe−N4−C40	125.6(3)	126.3(3)	125.8(3)
Fe−N4−C44	116.0(4)	112.5(3)	116.0(3)
C40−N4−C44	118.2(4)	118.4(4)	118.2(4)
C35−N5−C45	111.4(4)	109.0(4)	108.4(4)
C50−N5−C45	106.4(4)	109.5(3)	108.9(4)
Fe−N5−C35	109.3(3)	111.3(2)	109.6(3)
Fe−N5−C50	115.1(3)	114.8(3)	113.3(3)
Fe−N5−C45	105.3(4)	102.2(3)	105.5(3)
C35−N5−C50	109.3(4)	109.7(4)	110.8(4)
Fe−N6−C52	115.0(3)	117.2(3)	117.9(3)
N3−C30−C31	122.5(5)	122.1(4)	122.5(5)
C30−C31−C32	117.8(6)	119.0(5)	118.3(5)
C31−C32−C33	120.4(5)	119.6(5)	119.8(5)
C32−C33−C34	119.1(5)	118.7(5)	118.9(5)
N3−C34−C33	120.8(5)	122.2(4)	122.0(4)
N3−C34−C35	118.9(4)	116.6(4)	116.9(4)
C33−C34−C35	120.1(5)	121.1(4)	120.9(4)
C34−C35−N5	114.7(5)	113.4(4)	115.0(4)
N4−C40−C41	122.6(6)	122.4(5)	122.3(5)
C40−C41−C42	119.2(7)	119.3(5)	119.5(5)
C41−C42−C43	119.0(6)	119.3(5)	118.5(5)
C42−C43−C44	119.0(6)	118.7(5)	119.6(5)
N4−C44−C43	121.9(6)	121.8(4)	121.8(5)
N4−C44−C45	116.2(4)	115.1(4)	115.3(4)
C43−C44−C45	121.8(5)	123.1(4)	122.9(4)
N5−C45−C44	113.6(5)	111.3(3)	111.1(4)
N5−C50−C51	115.9(4)	113.8(4)	114.2(4)
C50−C51−C52	115.7(6)	115.4(5)	114.7(5)
C51−C52−N6	112.6(4)	112.0(5)	112.2(5)

[a] Estimated standard deviations in the least significant digits are given in parentheses.

Table 5. Interatomic Distances (Å) and Angles (deg) for the Hydrogen-Bonding Interactions for *fac*-[Fe(DPPA)(NCS)$_2$] in Polymorphs A−C[a]

D−H···A	D−H	H···A	D···A	D−H···A
		Polymorph A		
N6−H61···S1[b]	1.02(5)	2.72(4)	3.704(5)	164(4)
		Polymorph B		
N6−H61···S2[c]	0.98(4)	2.52(4)	3.493(4)	171(4)
		Polymorph C		
N6−H62···S1[d]	1.04(4)	2.96(4)	3.704(4)	129(4)

[a] Estimated standard deviations in the least significant digits are given in parentheses. [b] Symmetry operation: N6···S1, $+x, +y, +z - 1$. [c] Symmetry operation: N6···S2, $+x, -y + 1/2, +z + 1/2$. [d] Symmetry operation: N6···S1, $+x + 1/2, +y, -z + 1/2$.

the corresponding bond lengths are different in the two structures. The Fe−N distances involving the pyridine (Fe−N3 = 2.251(4) Å, Fe−N4 = 2.208(3) Å) and amino aliphatic

Table 6. Intermolecular Contacts (Å) for *fac*-[Fe(DPPA)$(NCS)_2$] in Polymorphs A−C[a]

atoms	sym operators	translations	dist
	Polymorph A		
S1···N6	$-x, -y, -z$	101	3.523(5)
S1···C52	$-x, -y, -z$	101	3.713(6)
S2···C33	$+x, +y, +z$	101	3.800(6)
S2···C43	$+x, +y, +z$	101	3.452(5)
C2···C33	$+x, +y, +z$	101	3.514(7)
C30···C30	$-x, -y, -z$	000	3.393(6)
C30···C31	$-x, -y, -z$	000	3.501(7)
C43···C42	$-x, -y, -z$	011	3.578(7)
	Polymorph B		
S1···C41	$-x, -y, -z$	100	3.680(6)
S2···N3	$+x, -y + 1/2, +z - 1/2$	000	3.764(4)
S2···C30	$+x, -y + 1/2, +z - 1/2$	000	3.729(5)
S2···C31	$-x, +y + 1/2, -z + 1/2$	100	3.701(6)
S2···C32	$-x, +y + 1/2, -z + 1/2$	100	3.726(6)
S2···C43	$+x, +y, +z$	100	3.658(5)
C2···N3	$+x, -y + 1/2, +z - 1/2$	000	3.588(5)
C2···C42	$+x, +y, +z$	100	3.490(7)
C31···C31	$-x, -y, -z$	101	3.532(7)
C33···N4	$+x, -y + 1/2, +z + 1/2$	000	3.560(6)
C33···C44	$+x, -y + 1/2, +z + 1/2$	000	3.453(7)
	Polymorph C		
S1···C30	$+x + 1/2, +y, -z + 1/2$	000	3.572(5)
S1···C31	$-x, +y + 1/2, -z + 1/2$	100	3.687(6)
S1···C32	$-x, +y + 1/2, -z + 1/2$	100	3.656(6)
S1···C51	$+x, +y, +z$	100	3.755(6)
S1···C52	$+x, +y, +z$	100	3.707(6)
S2···C50	$+x + 1/2, -y + 1/2, -z$	000	3.677(5)
S2···C42	$-x, -y, -z$	100	3.761(6)
C2···C35	$-x + 1/2, +y + 1/2, +z$	000	3.497(7)
C41···C52	$-x + 1/2, +y - 1/2, +z$	000	3.545(9)
C43···C43	$-x, -y, -z$	100	3.483(8)

[a] Estimated standard deviations in the least significant digits are given in parentheses.

(Fe−N5 = 2.250(4) Å, Fe−N6 = 2.162(4) Å) nitrogens are again longer than the Fe−N(CS) distances (Fe−N1 = 2.061(4) Å, Fe−N2 = 2.128(4) Å). The N−Fe−N angles between the *cis* nitrogens are in the range 76.9(1)−96.6(2)°, and those between the *trans* nitrogens are in the range 167.3(2)−169.9(2)°. As in the case of polymorph A the most reduced N−Fe−N angles are observed in the five-membered rings and between the two pyridine nitrogen atoms. The N−Fe−N angle in the amino aliphatic ring is close to 90°. The angles involving the thiocyanate N1 atom are larger than 90°. In spite of some differences in the corresponding distances and angles the general character of the $[FeN_6]$ core distortion due to the coordination of DPPA is similar for polymorphs A and B. The mode of coordination of the two thiocyanate groups is also similar in both polymorphs: the NCS groups are almost linear while the Fe−N−C linkages are bent (Fe−N1−C1 = 170.8(4)°, Fe−N2−C2 = 163.4(3)°). The pyridine containing N4 is nearly planar (mean plane $0.1456x + 0.3394y - 0.9293z = -0.3186$, the largest deviation being 0.010 Å for C44), whereas the pyridine containing N3 is appreciably bent (mean plane $-0.4734x + 0.0261y - 0.8805z = -6.0409$; the largest deviations are observed for N3 (0.012 Å), C31 (0.012 Å), and C34 (0.018 Å)). The dihedral angle between two pyridinic planes is much smaller (40.7(1)°) in polymorph B than in A.

Figure 2b shows a stereoview of the crystal lattice for polymorph B. The packing consists of chains of molecules parallel to the *c* axis. Within the chains the cohesion is due to weak hydrogen bonds between H61 (attached to N6) and the thiocyanate S2 atom of an adjacent molecule along the *c* axis. Between the chains, in the *a* and *b* directions, the cohesion is achieved by van der Waals interactions. Detailed information on the hydrogen-bonding interactions and the intermolecular distances for polymorph B are listed in Tables 5 and 6, respectively.

(d) Crystal Structure of Polymorph C. This form crystallizes in the orthorhombic *Pbca* space group. The unit cell contains four pairs of enantiomeric *fac*-[Fe(DPPA)$(NCS)_2$] molecules **2** ($Z = 8$). The perspective view of the molecule is shown in Figure 3a. Fractional atomic coordinates and selected bond lengths and angles are listed in Tables 2−4, respectively.

The $[FeN_6]$ octahedron is distorted in a similar way as in polymorphs A and B. The Fe−N distances including the pyridine (Fe−N3 = 2.213(3) Å, Fe−N4 = 2.197(4) Å) and amino aliphatic (Fe−N5 = 2.266(4) Å, Fe−N6 = 2.208(4) Å) nitrogens of DPPA are larger than the Fe−N(CS) distances (Fe−N1 = 2.067(5) Å, Fe−N2 = 2.112(4) Å). The N−Fe−N angles fall within 74.9(1)−97.9(2)° between adjacent nitrogens and 167.3(2)−167.6(2)° between opposite ones. The largest decrease from 90° of the N−Fe−N angles in polymorph C are once again observed in the five-membered rings. On the contrary, the N3−Fe−N4 angle involving the pyridine ligands, which is significantly reduced in polymorphs A and B (ca. 80°), is close to 90° in C. The NCS groups are almost linear whereas the Fe−N−C angles are bent (Fe−N1−C1 = 169.4(4)°, Fe−N2−C2 = 158.6(4)°).

A significant feature of this polymorph is found in the weak but distinct nonplanarity of the two pyridine rings, which suggests the existence of strain in the packing. For the ring containing N3 (mean plane $0.5919x - 0.7749y - 0.2217z = -0.2737$) the largest deviations from the mean plane are observed for N3 (0.011 Å), C30 (0.010 Å), and C34 (0.014 Å). For the ring containing N4 (mean plane $0.4812x + 0.6987y - 0.5294z = 0.4076$), the largest deviations are found for C43 (0.014 Å) and C44 (0.017 Å). The dihedral angle between the two pyridine rings in polymorph C is 82.0(2)°.

Figure 3b displays a stereoview of the crystal structure of polymorph C. The packing consists of layers of molecules parallel to the *ab* plane. In a layer, the cohesion is due to weak hydrogen bonds and numerous intermolecular interactions between the molecules. The H-bond pattern involves H62 (of N6) which is linked to the thiocyanate S1 atom of an adjacent molecule. The cohesion between the layers (in the *c* direction) is achieved by van der Waals contacts such as C43···C43 (pyridine rings), S2···C50, and S2···C42. Data on H-bonds and intermolecular distances are listed in Tables 5 and 6, respectively.

Magnetic Susceptibility Data. The magnetic properties of the three polymorphs were measured in both cooling and warming modes in order to detect thermal hysteresis effects.

(a) Polymorph A. The variation of the product of the molar magnetic susceptibility and the temperature $\chi_M T$ versus T for polymorph A is shown in Figure 4. At 295 K, the magnitude of $\chi_M T$ is 3.73 $cm^3\ mol^{-1}$ K ($\mu_{eff} = 5.46\ \mu_B$) and corresponds to a quintet spin state. On cooling, a slow decrease of $\chi_M T$ is observed down to 210 K and then a gradual spin transition ending at around 150 K occurs. The transition temperature $T_{1/2}$ (temperature for which the high-spin fraction is equal to 0.5) is 176 K. Upon further cooling of the sample to 10 K, the value of $\chi_M T$ attains 0.03 $cm^3\ mol^{-1}$ K ($\mu_{eff} = 0.49\ \mu_B$) which is close to the expected temperature-independent paramagnetism value for low-spin iron(II) complexes. The absence of residual paramagnetism at low temperature evidenced by Mössbauer spectroscopy (vide infra) as well as the closeness of the experimental $\chi_M T$ to the expected value for a pure singlet spin state suggest that the spin transition is practically complete. The same magnetic behavior was observed in the warming mode. No thermal hysteresis effect was observed for this gradual spin

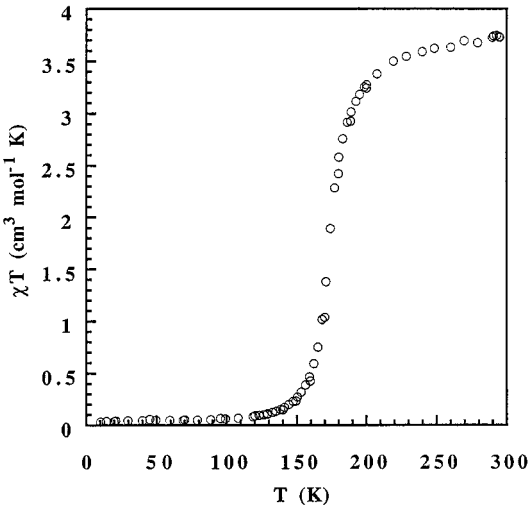

Figure 4. Thermal variation of $\chi_M T$ for *fac*-[Fe(DPPA)(NCS)$_2$] in polymorph A.

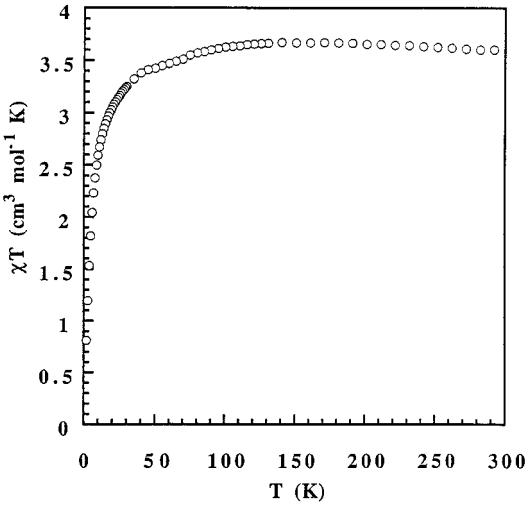

Figure 5. Thermal variation of $\chi_M T$ for *fac*-[Fe(DPPA)(NCS)$_2$] in polymorph B.

transition of polymorph A between high-spin ($S = 2$) and low-spin ($S = 0$) electronic states.

(b) Polymorph B. For this polymorph the magnitude of $\chi_M T$ at 295 K is 3.58 cm^3 mol^{-1} K ($\mu_{eff} = 5.35\ \mu_B$) featuring a quintet spin state (Figure 5). On cooling, $\chi_M T$ remains nearly constant down to 70 K. Below this temperature, the $\chi_M T$ product begins to decrease slowly and finally attains a value of 0.81 cm^3 mol^{-1} K at 2 K. The temperature-dependent decrease of the $\chi_M T$ value in the low-temperature region indicates the presence of zero-field splitting of the high-spin iron(II) ground state.

(c) Polymorph C. The magnetic properties of polymorph C is shown in Figure 6. The $\chi_M T$ product at 190 K is equal to 3.15 cm^3 mol^{-1} K ($\mu_{eff} = 5.02\ \mu_B$). This characteristic value for high-spin iron(II) complexes remains almost constant upon cooling to 114 K, and then a very abrupt HS ⇔ LS transitions occurs within 7 K. At 100 K, $\chi_M T$ attains 0.12 cm^3 mol^{-1} K ($\mu_{eff} = 0.98\ \mu_B$), which is typical for low-spin iron(II) species. In the warming mode a very abrupt spin transition is observed between 116 and 121 K. Polymorph C exhibits a very abrupt and complete spin transition between high-spin ($S = 2$) and low-spin ($S = 0$) states with transition temperatures $T_c\downarrow = 112$ K and $T_c\uparrow = 120$ K in the cooling and warming modes, respectively, and a hysteresis width equal to 8 K.

Mössbauer Spectroscopy. (a) Polymorph A. The temperature dependence of the ^{57}Fe Mössbauer spectra of polymorph A was studied between 80 and 295 K. Figure 7 shows four

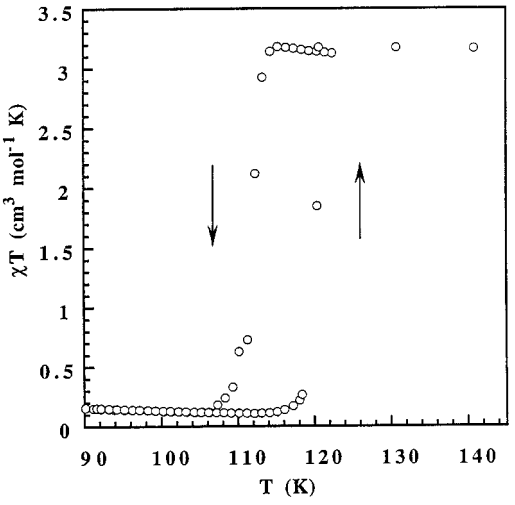

Figure 6. Thermal variation of $\chi_M T$ for *fac*-[Fe(DPPA)(NCS)$_2$] in polymorph C.

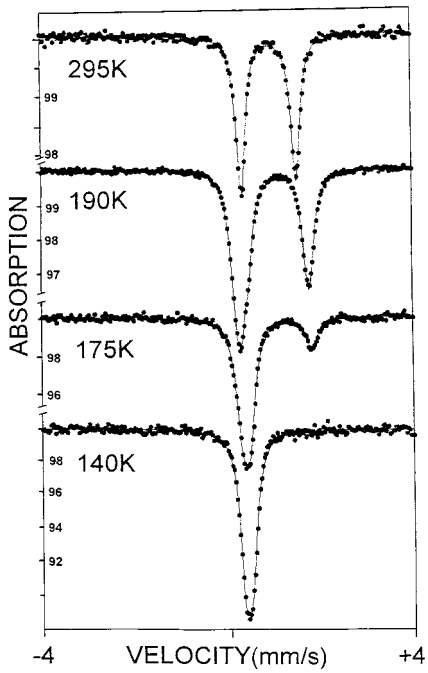

Figure 7. Selected Mössbauer spectra of *fac*-[Fe(DPPA)(NCS)$_2$] in polymorph A recorded in the cooling mode. The solid lines represent fitted curves.

representative spectra selected from a series of increasing temperature measurements. The main doublets observed at high and low temperature are typical for iron(II) high-spin and low-spin states, respectively. Relevant values of the Mössbauer parameters as a function of temperature are gathered in Table 7. The isomer shift (IS(HS) = 0.987(1) and IS(LS) = 0.513(1) mm s^{-1}) and quadrupole splitting values (ΔE_Q(HS) = 1.148(2) and ΔE_Q(LS) = 0.168(3) mm s^{-1}) at 295 and 80 K are in line with previously observed values for iron(II) spin-crossover compound.[1b] At intermediate temperatures the spectra show the co-existence of the two spin isomers with strongly temperature-dependent relative intensities. No spectrum deformation or line broadening was observed in this temperature range (80−295 K), indicating that the LS ⇔ HS conversion rates are slow compared to the hyperfine frequencies (∼10^8 s^{-1}).[17] At 80 K, the Mössbauer spectrum did not detects any residual high-spin species while the fitting of the 295 K spectrum indicated the presence of ∼6% of low-spin complex.

(17) (a) Adler, P.; Hauser, A.; Vefn, A.; Spiering, H.; Gütlich, P. *Hyperfine Interact.* **1989**, *47*, 343. (b) Adler, P.; Spiering, H.; Gütlich, P. J. *Chem. Phys. Lett.* **1994**, *226*, 289.

Table 7. Least-Squares-Fitted Mössbauer Data[a,b] for *fac*-[Fe(DPPA)(NCS)$_2$] in Polymorph A

	low-spin state			high-spin state			
T (K)	IS (mm s^{-1})	ΔE_q^{LS} (mm s^{-1})	$\Gamma/2$ (mm s^{-1})	IS (mm s^{-1})	ΔE_q^{HS} (mm s^{-1})	$\Gamma/2$ (mm s^{-1})	A_{HS}/A_{tot} (%)
80	0.513(1)	0.168(3)	0.144(2)				0
140	0.500(1)	0.152(2)	0.124(2)				0
170	0.480(2)	0.169(3)	0.125(2)	1.183(8)	1.37(2)	0.13(1)	16
175	0.462(2)	0.185(4)	0.136(2)	1.173(5)	1.37(1)	0.133(7)	28
190	0.473(2)	0.147(3)	0.111(3)	1.053(1)	1.513(2)	0.141(2)	69
275	0.37(2)	*0.17*	0.134(2)	1.000(1)	1.201(2)	0.134(2)	92
295	0.39(2)	*0.17*	0.115(1)	0.987(1)	1.148(2)	0.155(1)	94

[a] IS, isomer shift; ΔE_q, quadrupole splitting; Γ, half-height width of line; A_{HS}/A_{tot}, area ratio. [b] With their statistical standard deviations given in parentheses; italicized values were fixed to the fit; isomer shift values refer to metallic iron at 300 K. *A*: base-line-corrected data area.

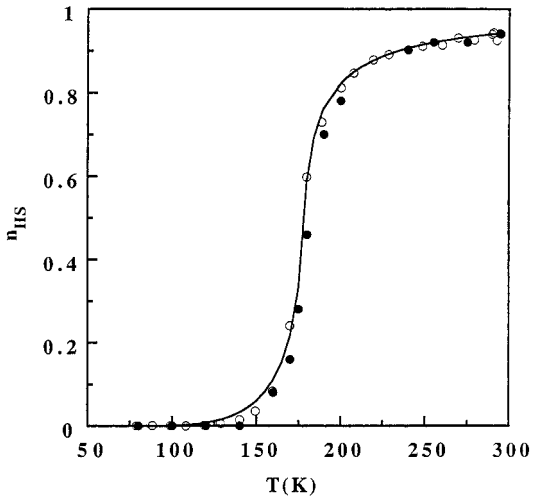

Figure 8. Thermal variation of the high-spin fraction (n_{HS}) of *fac*-[Fe(DPPA)(NCS)$_2$] in polymorph A. Open and black circles correspond to magnetic susceptibility and to Mössbauer spectroscopy data, respectively. The solid line represents least-squares fit with the two-level Ising-like model.

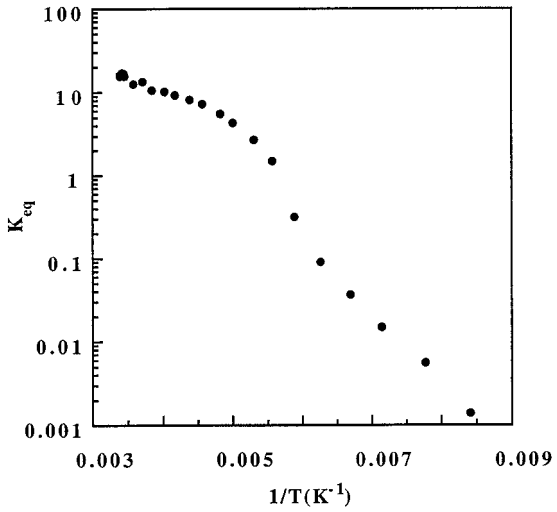

Figure 9. Arrhenius plot of the equilibrium constant obtained by Mössbauer spectroscopy for *fac*-[Fe(DPPA)(NCS)$_2$] in polymorph A.

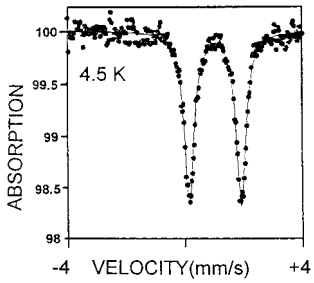

Figure 10. Selected Mössbauer spectrum of *fac*-[Fe(DPPA)(NCS)$_2$] in polymorph B at 4.5 K. The solid lines represent fitted curves.

The n_{HS} value estimated from the magnetic susceptibility data were calibrated with the 293 K $n_{HS}(\sim A_{HS}/A_{tot})$ value obtained from the Mössbauer measurements. The temperature dependence of n_{HS} derived from the magnetic susceptibility data and the Mössbauer study is displayed in Figure 8. As can be seen the results provided by both methods are in a good agreement. The spin conversion in polymorph A is rather gradual and essentially achieved between 160 and 210 K. The transition temperature ($T_{1/2} = 178$ K) found from Mössbauer spectroscopy is close to that (176 K) derived from magnetic measurements.

The theoretical curve obtained by a least-square fit of the n_{HS} Mössbauer data with the mean field equation of the two level Ising-like model[18] formally equivalent to the macroscopic models[19] is shown in Figure 8. The fitted values for the parameters include the energy gap between the HS and LS electronic states $\Delta_{eff} = E_{HS} - E_{LS} = 824$ K, the ferromagnetic-like intermolecular coupling parameter (cooperativity parameter)[18] $J_{coop} = 160$ K, and the ratio of effective degeneracies of electron-vibrational levels[19] $r_{eff} = g_{HS}/g_{LS} = 102$. Using the formal relationship between the macroscopic (entropy and enthalpy) and microscopic parameters (Δ_{eff} and r_{eff}),[19] the molar entropy and enthalpy changes upon spin state conversion were calculated to be $\Delta S = R \ln r_{eff} = 39$ J K^{-1} mol^{-1} and $\Delta H = N\Delta_{eff} = 6.9$ kJ mol^{-1}. The estimated values of the entropy and enthalpy variations fall within the limits found from calorimetric measurements for mononuclear iron(II) spin transition compounds.[1e,g] Interestingly, the ratio $J_{coop}/T_{1/2}$ (ca. 0.9) suggests that some cooperativity exists in the spin transition of polymorph A (this ratio would be equal to 1 for a first-order spin transition with thermal hysteresis).[20] This conclusion is supported by the reversed S-shaped curve of the Arrhenius plot of the equilibrium constant ($K_{eq} = n_{HS}/(1 - n_{HS})$) obtained from Mössbauer spectroscopy (Figure 9).[21]

(b) Polymorph B. The ^{57}Fe Mössbauer spectra of B were recorded at 4.5, 80, and 300 K. The main doublets observed at these temperatures are typical of a iron(II) high-spin ground state. Figure 10 shows the spectrum obtained at 4.5 K. The isomer shift (IS = 1.134(2) mm s^{-1}) and quadupole splitting ($\Delta E_Q = 1.700(5)$ mm s^{-1}) are consistent with earlier data for iron(II) high-spin compounds. Thus the Mössbauer spectra are in line with the above discussed magnetism measurements and confirm that, whatever the temperature, complex **2** is high-spin in polymorph B.

(c) Polymorph C. The Mössbauer spectra of polymorph C were recorded between 80 and 295 K. Figure 11 shows relevant

(18) Bousseksou, A.; Nasser, J.; Linares, J.; Boukheddaden, K.; Varret, F. *J. Phys. 1 (Paris)* **1992**, *2*, 1381.
(19) (a) Bousseksou, A.; Nasser, J.; Linares, J.; Boukheddaden, K.; Varret, F. *Mol. Cryst. Liq. Cryst.* **1993**, *243*, 269. (b) Bousseksou, A. Ph.D. Thesis, Université Paris 6, 1992. (c) Bousseksou, A.; Constant-Machado, H.; Varret, F. *J. Phys. 1 (Fr.)* **1995**, *5*, 747.
(20) Wajnflasz, J.; Pick, R. *J. Phys.-C* **1971**, *32*, 1.
(21) Lemercier, G.; Bousseksou, A.; Seigneuric, S.; Varret, F.; Tuchagues, J. P. *Chem. Phys. Lett.* **1994**, *226*, 289.

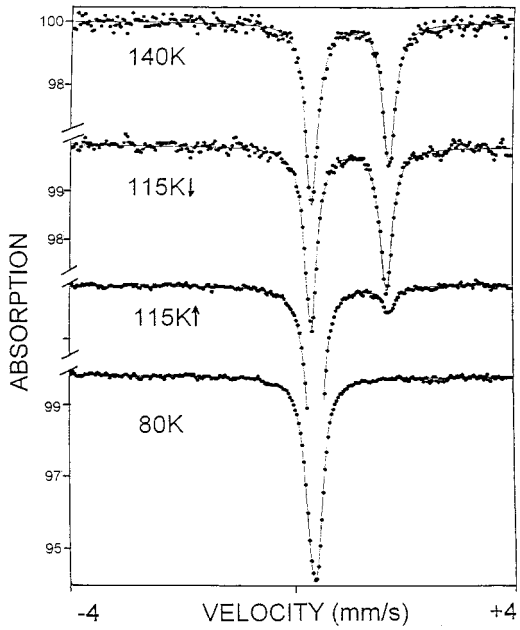

Figure 11. Selected Mössbauer spectra of *fac*-[Fe(DPPA)(NCS)$_2$] in polymorph C in the cooling and warming modes. The solid lines represent fitted curves.

spectra at 140, 115, and 80 K (decreasing temperature) and at 115 K (increasing temperature). Between 295 and 140 K the observed doublets are typical of high-spin iron(II) ($S = 2$). This is in line with the isomer shift and quadrupole splitting values at 140 K, 1.099(1) and 1.312(2) mm s^{-1}, respectively. The Mössbauer spectrum of C at 115 K (decreasing temperature regime) could be fitted by two doublets featuring high-spin and low-spin states (see Table 8). In the cooling mode, the n_{HS} fraction at 115 K could thus be estimated at 98(1)%. The dissymmetry of the high-spin quadrupole doublets at 140 and 115 K is due to a weak texture effect (the average angle between the γ-ray direction and the z crystallographic axis of the sample is 60°). In the spectrum recorded at 80 K, IS = 0.509(1) mm s^{-1} and $\Delta E_Q = 0.125(1)$ mm s^{-1}. These figures correspond to a $S = 0$ low-spin ground state of iron(II). In the warming mode at 115 K the spectrum again contains two doublets corresponding to the high-spin and low-spin states, but in this case the n_{HS} fraction was evaluated at 19.0(4)%. These observations clearly show that complex **2** in polymorph C undergoes a complete, thermally induced spin transition between high-spin ($S = 2$) and low-spin ($S = 0$) ground states. The inequality of the n_{HS} fraction observed at 115 K in the cooling and warming modes confirms that the spin transition in polymorph C is attended with hysteresis, as evidenced by the magnetic measurements.

Discussion

This work was initially undertaken to study how strain effects due to the size of chelate rings could modify the spin-crossover regime of iron(II) complexes. In the complex *mer*-[Fe(DPEA)(NCS)$_2$] (**1**) reported previously[8] the DPEA ligand is coordinated to the metal by two pyridine nitrogens in apical position and two aliphatic amino groups in adjacent position in the [FeN$_6$] octahedron, forming three five-membered metallocycles. The X-ray analysis of **1** has revealed the existence of an important distortion of the [FeN$_6$] core from O_h symmetry, which has been ascribed to sterical constraints due to the tetradentate ligand. The spin conversion observed in **1** at 138 K being close to a first-order transition, we anticipated that suitable changes in the structure of the ligand, which would release some strain, could modify the magnetic properties and possibly lead to spin transition with hysteresis. This is why we synthesized the DPPA ligand, differing from DPEA by the presence of an additional methylene unit in the amino aliphatic chain. Upon coordination to iron(II), DPPA can form one six-membered and two five-membered chelate rings. It has been reported that the expansion of a five-membered to a six-membered chelate ring, despite some weakening of the ligand field, favors low-spin states due to the reduction of steric strain.[1d]

Things, however, did not exactly follow the above expectations. First, during the preparation of the iron(II) DPPA complex, we did not isolate a single-crystal form but four different species. Three of these were polymorphic modifications, and the fourth one was a solvated complex.[10] Second, the *mer* configuration **1** has been isolated for the [Fe(DPEA)(NCS)$_2$] complex, whereas the three polymorphs of [Fe(DPPA)(NCS)$_2$] feature the *fac* configuration **2**. This circumstance, which made a direct comparison of the effect of metallocycle strain on magnetic properties irrelevant, offered instead a valuable opportunity to focus on the consequence of polymorphism on the magnetic properties of the same complex.

Only few manifestations of polymorphism are known among spin transition systems. The polymorphism of [Fe(phen)$_2$(NCS)$_2$][2] and of [Fe(bipy)$_2$(NCS)$_2$][3] has been the object of a number of studies since the 60s. Two crystal forms have been found for the former and three for the latter, depending on the preparation procedure. All forms of both compounds display HS ⇔ LS transitions. The different polymorphs are distinguished by the abruptness of the spin transition and by the value of the residual paramagnetism at low temperature. Unfortunately, only incomplete X-ray structural data are available for the two polymorphs of [Fe(bipy)$_2$(NCS)$_2$],[3,22] and among the two polymorphic modifications of [Fe(phen)$_2$(NCS)$_2$], only one was fully characterized by X-ray crystallographic study.[16a] Sacconi et al. have obtained two unsolvated forms of [FeCl$_2$(Ph$_2$PCH=CHPPh$_2$)$_2$] and one of its acetone solvate.[23] The unsolvated forms remain in the high-spin state down to 90 K whereas the solvate undergoes a spin transition at ~230 K.

To our knowledge the only case of polymorphism where two nonsolvated crystal forms display drastically different magnetic behaviors has been documented by McGarvey et al.[4] Polymorph I of [Fe(bt)$_2$(NCS)$_2$] shows a HS ⇔ LS transition with a hysteresis,[24] while II is high spin over the temperature range 77−300 K. The X-ray analysis of both forms, which crystallize in the same space group, revealed some small but significant differences between the two structures. In polymorphs I and II the average Fe−N distances are 2.158 and 2.175 Å, respectively, and a more effective network of intermolecular interactions has been found in polymorph I than in II.

The [Fe(DPPA)(NCS)$_2$] complex studied here provides a further, particularly striking example, of a spin transition system in which polymorphism leads to qualitatively different magnetic properties. The X-ray structural characterization discussed above shows that the [FeN$_6$] core is distorted in a similar fashion and that the mean Fe−N distances are almost identical in the three polymorphic modifications (2.174, 2.177, and 2.177 Å, in A−C, respectively). The first coordination sphere of iron(II) contains three pairs of functionally distinct nitrogen atoms, namely, of thiocyanate, aliphatic, and aromatic types, which we will now consider separately. The small observed differences in the average Fe−N(CS) distances (2.094, 2.095, and 2.090 Å in A−C, respectively) are not significant. However, unlike other

(22) König, E.; Watson, K. J. *Chem. Phys. Lett.* **1970**, *6*, 457.
(23) Cecconi, F.; Di Vaira, M.; Midollini, S.; Orlandini, A.; Sacconi, L. *Inorg. Chem.* **1981**, *20*, 3423.
(24) (a) Bradley, G.; McKee, V.; Nelson, S. M. *J. Chem. Soc., Dalton Trans.* **1978**, 522. (b) Müller, E. W.; Spiering, H.; Gütlich, P. *J. Chem. Phys.* **1983**, *79*, 1439.

Table 8. Least-Squares-Fitted Mössbauer Data[a,b] for *fac*-[Fe(DPPA)(NCS)$_2$] in Polymorph C

	low-spin state			high-spin state			
T (K)	IS (mm s^{-1})	ΔE_q^{LS} (mm s^{-1})	$\Gamma/2$ (mm s^{-1})	IS (mm s^{-1})	ΔE_q^{HS} (mm s^{-1})	$\Gamma/2$ (mm s^{-1})	A_{HS}/A_{tot} (%)
140↓				1.099(1)	1.312(2)	0.128(2)	100
115↓	*0.502*	*0.118*	0.129(2)	1.113(2)	1.359(3)	0.129(2)	98(1)
80↓	0.509(1)	0.118(2)	0.125(1)				0
115↑	0.502(2)	*0.118*	0.126(1)	*1.113*	*1.359*	0.126(5)	19.0(4)

[a] IS, isomer shift; ΔE_q, quadrupole splitting; Γ, half-height width of line; A_{HS}/A_{tot}, area ratio. [b] With their statistical standard deviations given in parentheses; underlined values were fixed to the fit; isomer shift values refer to metallic iron at 300 K. *A*: base-line-corrected data area.

biisothiocyanate complexes of mono- and bidentate ligands,[4,16,22,25] in each polymorph the two Fe−N(CS) distances are different (ca. 2.07 Å vs ca. 2.11 Å; see Table 3). This is due to the fact that the N1(CS) ligand being less sterically hindered can approach the metal center closer than the N2(CS) one. The mean Fe−N(aromatic) distances are close to one another in polymorphs A (2.196 Å) and C (2.205 Å) whereas it is significantly longer in B (2.230 Å). The difference between the two Fe−N(aromatic) distances is smaller in polymorph A and C than in B where Fe−N3 is 0.043 Å longer than Fe−N4 (see Table 3). For the Fe−N(aliphatic) distances the trend is opposite to that of the Fe−N(aromatic) ones. The shortest mean Fe−N(aliphatic) distance is found for polymorph B (2.206 Å), and the longest distances are found for A and C (2.233 and 2.237 Å, respectively). In the three polymorphs the tertiary N5 nitrogen is more remote from the metal than the primary N6 one, which is certainly due to steric reasons.

In summary, the above comparison of the Fe−N distances shows that the most significant differences between polymorphs A and C (spin transition) and B (high-spin) appear in the mean value of Fe−N(aromatic) distances (longer in B) and Fe−N(aliphatic) ones (shorter in B).

We now address the question of the effect of small structural variations on the ligand field strength which in the present system is certainly close to a critical value. The ligand field strength normally depends on the metal−ligand distance (as $\sim 1/r^5$) and on the nature of the donor atoms. In the [FeN$_6$] core, the ligand field produced by the aromatic nitrogens contains σ and π contributions and is stronger than that caused by the aliphatic nitrogen ligands, which is entirely determined by σ interactions.[1d] In principle, the stronger field of aromatic ligands favors low-spin states, and most iron(II) complexes of aliphatic ligands exhibit high-spin ground states. In polymorph B the mean Fe−N(aromatic) distances are longer than in A and C, which certainly causes a decrease of the ligand field, not totally compensated by the increase due to the shortening of the Fe−N(aliphatic) distances. Thus we explain the purely high-spin character of complex **2** in polymorph B by an overall weakening of the ligand field strength mostly due to the longer Fe−N(aromatic) distances.

As mentioned above, the longer mean Fe−N(aromatic) distance in polymorph B is mainly due to the unusually long Fe−N3 distance (2.251 Å), the Fe−N4 distance (2.208 Å) being close to the corresponding distances in A and C (2.182−2.213 Å). This stretching of Fe−N3 in B seems to originate from the presence of strained regions between adjacent molecules in the chains parallel to the *c* axis (symmetry operations: $+x, -y + {}^1/_2, +z + {}^1/_2$; $+x, -y + {}^1/_2, +z - {}^1/_2$). The first strained region involves the N3-containing pyridine ring and the N2C2S2 ligand of an adjacent molecule, and more precisely the following contacts: N3···C2 (3.59 Å), N3···S2 (3.76 Å), and C30···S2 (3.73 Å). The second center of strain occurs between the N3- and N4-containing pyridine rings of neighboring molecules in a column. This strain is revealed by the important deviation from planarity of the N3 containing pyridine ring and is associated with the existence of two short contacts, C33···C44 (3.45 Å) and C33···N4 (3.56 Å), which possibly account for the reduction of the dihedral angle between the pyridine planes of the ligand (40.7° in B compared with 70.7 and 82° in A and C, respectively).

The magnetic measurements show that the HS ⇔ LS transition takes place at about 176 K for polymorph A and at 112 and 120 K in the cooling and warming modes, respectively, for C. This large difference in the transition temperatures suggests that the ligand field is weaker in C than in A, and this explanation is again consistent with the observation that the mean Fe−N(aromatic) distances are longer in C than in A. The hysteresis loop observed for polymorph C shows that the spin conversion is associated with a first-order phase transition, which in turn requires an excellent cooperativity of the molecular contacts to ensure the reversibility of the process when the temperature variation is reversed. As the Arrhenius plot of Figure 9 and the value of $J_{coop}/T_{1/2}$ (0.9) show, the spin transition in polymorph A itself is also attended with some cooperativity and is probably not far from being first-order like is C. As said above, the crystal packing of A and C consist of layers of molecules. Within the layers, the molecules are connected by H-bonds of the same length in the two polymorphs and by several short intermolecular contacts. In polymorph A, the cohesion between the layers is mainly due to van der Waals interactions between the pyridine rings (contact C42···C43). In polymorph C, similar contacts exist (C43···C43), and these is the presence of two additional contacts (S2···C50 and S2···C42) which probably makes the interactions between layers more efficient, resulting in a better cooperativity eventually leading to hysteresis.

Acknowledgment. We are grateful to the CNRS, Département des sciences chimiques, for a grant to G.M. We thank J.-F. Meunier for technical assistance in the Mössbauer spectroscopy measurements.

Supporting Information Available: A full presentation of crystallographic data and experimental parameters for three polymorphs A−C of [Fe(DPPA)(NCS)$_2$] (Table S1), general displacement parameter expressions (*U*'s) (Table S2), positional parameters for the hydrogen atoms (Table S3), bond distances and angles (Tables S4 and S5, respectively), and least-squares planes (Table S5) (14 pages). Ordering information is given on any current masthead page.

IC971174T

(25) (a) Roux, C.; Zarembowitch, J.; Gallois, B.; Granier, T.; Claude, R. *Inorg. Chem.* **1994**, *33*, 2273. (b) Real, A.; Zarembowitch, J.; Kahn, O.; Solans, X. *Inorg. Chem.* **1987**, *26*, 2939.